



Supramolecular host–guest coordination systems:
 $[(G^+)(Me_3E)_3M^{II}(CN)_6]_\infty$ as ion exchangers, where $(G^+ = Me_3E, Et_4N$ or $stp)$, $(E = Sn$ or $Pb)$ and $(M = Fe$ or $Ru)$

Amany M.A. Ibrahim*

Department of Chemistry, Faculty of Science, Ain Shams University, Cairo, Egypt

Received 5 February 1999; accepted 26 May 1999

Abstract

A number of 3D-coordination polymers, constructed via $[^dM(CN)_6]$ building blocks and (Me_3E) connecting units, have been prepared and characterized by X-ray powder diffraction and different spectroscopic methods. 1-Methyl-4-(4'-*R*-styryl) or (2'-*R*-styryl) pyridinium cations (*stp*) have been successfully encapsulated within the expandable wide channels of the 3D-coordination polymers by tribochemical or ion exchange reactions producing novel molecular composites. Apart from **6**, $[(4'-OCH_3-stp)(Me_3Sn)_3Fe^{II}(CN)_6-MeOH]_\infty$ which exhibits thermochromic behaviour, the molecular composites $[(stp)_x(Me_3E)_3Fe^{III}_xFe^{II}_{1-x}(CN)_6]_\infty$, **1–12** are mixed valence materials exhibiting localized interaction between the mixed valence iron. The results indicated an ion charge transfer interaction between the guest *stp*-cations and the host matrix. The molecular composites $[(stp)(Me_3E)_3M^{II}(CN)_6]_\infty$, **13–18** are due to the facile readiness of the coordination polymers $[(Me_3E)_4M(CN)_6]_\infty$ and $[(Et_4N)(Me_3Sn)_3Fe(CN)_6]_\infty$ to ion exchange. © 1999 Elsevier Science Ltd. All rights reserved.

Keywords: Coordination polymers; Molecular composites; Styryl pyridinium salts; Hexacyanometalate; Sn; Pb

1. Introduction

While the metal dichalcogenide [1,2] and FeOCl [3–8] materials have been extensively studied for many years as layered compounds, the 3D-supramolecular coordination polymers $[(R_3E)_nM(CN)_6]_\infty$ ($R = \text{alkyl or phenyl}$, $E = \text{Sn or Pb}$, $n = 3$ or 4 , $M = \text{Fe, Co, Ru or Os}$) have recently attracted much interest [9–15]. The polymers containing Fe and Co were successfully subjected to single-crystal X-ray studies leading to initial reinspection of the structure of the other polymeric homologues [12–15]. The non-superimposable 3D-networks of $[(Me_3E)_3M(CN)_6]_\infty$ involve distorted octahedral $[M(CN)_6]$ building blocks and Me_3E $(NC)_2$ connecting units of trigonal-bipyramidal (*tbp*) configuration. These polymers contain remarkably wide, practically parallel, channels whose walls are internally coated by constituents of the lipophilic Me_3E groups [12,13].

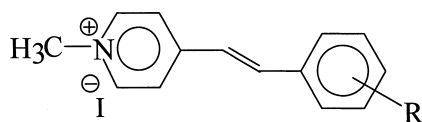
Although chemically very different from the dichalcogenides, $[(R_3E)_3Fe^{III}(CN)_6]_\infty$ systems are strong ox-

idizing materials [16], they show a quite analogous intercalation chemistry exhibiting a variety of interesting chemical properties, such as magnetic, conductive and optical characteristics. Thus, a considerable number of different Lewis bases [17–19] have been successfully encapsulated under comparatively mild reaction conditions. Also, the encapsulation of several organometallic guest molecules have been demonstrated [20,21]. On the other hand, the most outstanding chemical property of $[(Me_3E)_4M(CN)_6]_\infty$ polymers are their facile readiness to ion exchange [20–23].

The present study has been developed to synthesize and characterize novel host guest systems by encapsulating 1-methyl 4-(4'-*R*-styryl) or (2'-*R*-styryl) pyridinium cations (*stp*) within the channels of the 3D-coordination polymers $[(Me_3E)_3Fe^{III}(CN)_6]_\infty$ or by ion exchange reactions where the *stp*-cation can be introduced quantitatively into the channels of the negatively charged host-network $[(Me_3E)_3M^{II}(CN)_6]_\infty^-$.

The choice of *stp*-compounds (Scheme 1) is based on the wide applications of the stilbazolium salts in several areas. They are used as electrochromic compounds for

*Tel.: +20-2-260-1379; fax: +20-2-261-6474.



R = (1) 4'-H, (2) 4'-OH, (3) 4'-OCH₃, (4) 4'-NMe₃, (5) 4'-Cl,
(6) 4'-Br, (7) 4'-NO₂, (8) 2'-OH, (9) 2'-OCH₃

Scheme 1.

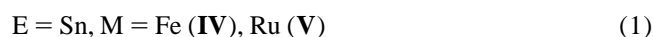
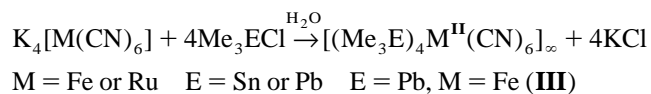
their membrane potentials and high voltage sensitivity [24], as fluorescence probes to follow the fast change of electrical membrane potential during an action potential in neurons [25] and in nonlinear optical laser frequency doublers and liquid crystals devices [25].

2. Experimental

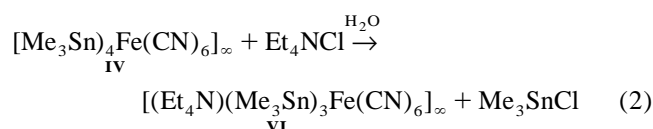
1-Methyl-4-(4'-R-styryl) or (2'-R-styryl) pyridinium iodides (stpi) were prepared by the base-catalysed aldol condensation of picolinium iodide with different aldehydes [26,27]. The purity and identity of (stpi), (Scheme 1) were checked by thin layer chromatography, elemental analysis and IR spectra. The stpi are in the *trans* form as long as the condensation reaction is carried out in the dark.

The 3D-coordination polymers [(Me₃Sn)₃Fe(CN)₆]_∞, **I**, and [(Me₃Pb)₃Fe(CN)₆]_∞, **II**, were obtained when aqueous solutions of trimethyltin chloride or trimethyllead chloride and K₃[Fe(CN)₆] are mixed in the dark under nitrogen

atmosphere in the molar ratio 3:1. The polymers [(Me₃E)₄M(CN)₆]_∞ were obtained as white precipitates upon the addition of an aqueous solution of Me₃SnCl or Me₃PbCl to K₄[M(CN)₆] in the molar ratio 4:1.



The polymer **IV** exchanges at most one (Me₃Sn⁺) cation for (Et₄N⁺) cation when exposed to an aqueous solution of Et₄NCl to give the polymer **VI**.



The purity and identity of these coordination polymers were checked by elemental analysis and vibrational spectra.

2.1. Preparation of the molecular composites

stp-Cations can be encapsulated within the channels of the coordination polymers **I** and **II** by mixing equimolar quantities of both, the stpi-salt and **I** or **II**. The mixture was wetted with few drops of water and ground smoothly for a long time to avoid the effect of heat on the

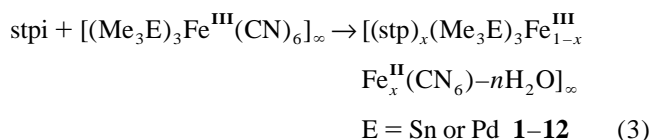
Table 1
Elemental analysis and colours of the molecular composites 1–12

No.	Molecular compositions	Colour	Elemental analysis, % Calc./(Found)			
			C	H	N	Fe
1	[(4'-H-stp) _{0.9} (Me ₃ Sn) ₃ Fe ^{III} Fe ^{II} _{0.9} (CN) ₆ -2H ₂ O] _∞	Buff	36.19 (36.00)	4.80 (4.83)	10.55 (10.31)	6.10 (5.92)
2	[(4'-H-stp) _{0.8} (Me ₃ Pb) ₃ Fe ^{III} Fe ^{II} _{0.8} (CN) ₆ -2H ₂ O] _∞	Yellow	27.08 (26.91)	3.66 (3.60)	8.20 (7.96)	4.81 (4.76)
3	[(4'-OH-stp) _{0.85} (Me ₃ Sn) ₃ Fe ^{III} Fe ^{II} _{0.85} (CN) ₆ -2H ₂ O] _∞	Orange	36.37 (36.51)	4.64 (4.56)	10.80 (10.70)	6.29 (6.23)
4	[(4'-OCH ₃ -stp) _{0.85} (Me ₃ Sn) ₃ Fe ^{III} Fe ^{II} _{0.85} (CN) ₆ -2H ₂ O] _∞	Yellow	36.48 (36.54)	4.70 (4.62)	10.50 (10.32)	6.11 (6.06)
5	[(4'-OCH ₃ -stp) _{0.8} (Me ₃ Pb) ₃ Fe ^{III} Fe ^{II} _{0.8} (CN) ₆ -2H ₂ O] _∞	Reddish brown	27.35 (27.23)	3.72 (3.69)	8.03 (7.87)	4.71 (4.62)
6	[(4'-OCH ₃ -stp)(Me ₃ Sn) ₃ Fe ^{II} (CN) ₆ -MeOH] _∞	Orange	38.72 (38.69)	4.93 (4.91)	10.19 (9.89)	5.81 (5.78)
7	[(4'-NMe ₂ -stp) _{0.85} (Me ₃ Sn) ₃ Fe ^{III} Fe ^{II} _{0.85} (CN) ₆] _∞	Brown	37.88 (37.81)	4.80 (4.90)	11.89 (11.72)	6.16 (6.10)
8	[(4'-Cl-stp) _{0.8} (Me ₃ Sn) ₃ Fe ^{III} Fe ^{II} _{0.8} (CN) ₆] _∞	Brown	35.44 (35.38)	4.25 (4.28)	10.73 (10.59)	6.29 (6.18)
9	[(4'-Br-stp) _{0.7} (Me ₃ Sn) ₃ Fe ^{III} Fe ^{II} _{0.7} (CN) ₆ -2H ₂ O] _∞	Grey	31.96 (31.83)	4.34 (4.38)	10.07 (10.00)	5.99 (5.81)
10	[(4'-NO ₂ -stp) _{0.75} (Me ₃ Sn) ₃ Fe ^{III} Fe ^{II} _{0.75} (CN) ₆ -H ₂ O] _∞	Green	33.94 (33.82)	4.33 (4.35)	11.64 (11.58)	6.19 (6.12)
11	[(2'-OH-stp) _{0.85} (Me ₃ Sn) ₃ Fe ^{III} Fe ^{II} _{0.85} (CN) ₆ -H ₂ O] _∞	Yellow	37.74 (37.80)	4.60 (4.62)	10.65 (10.51)	6.16 (6.12)
12	[(2'-OCH ₃ -stp) _{0.9} (Me ₃ Sn) ₃ Fe ^{III} Fe ^{II} _{0.9} (CN) ₆] _∞	Yellowish brown	36.37 (36.33)	4.64 (4.60)	10.80 (10.71)	6.29 (6.16)

Table 2
Elemental analysis and colours of the molecular composites **13–18**

No.	Molecular compositions	Colour	Elemental analysis, % Calc./(Found)			
			C	H	N	Fe
13	$[(4'\text{-H-stp})(\text{Me}_3\text{Sn})_3\text{Fe}(\text{CN})_6]_\infty$	Yellowish brown	38.72 (38.68)	4.59 (4.51)	10.88 (10.62)	6.21 (6.15)
14	$[(4'\text{-OCH}_3\text{-stp})(\text{Me}_3\text{Sn})_3\text{Fe}(\text{CN})_6]_\infty$	Yellow	38.76 (38.36)	4.66 (4.76)	10.55 (10.47)	6.01 (5.92)
15	$[(4'\text{-H-stp})(\text{Me}_3\text{Pb})_3\text{Fe}(\text{CN})_6]_\infty$	Brown	29.90 (29.70)	3.55 (3.38)	8.42 (8.32)	4.79 (4.61)
16	$[(4'\text{-OCH}_3\text{-stp})(\text{Me}_3\text{Pb})_3\text{Fe}(\text{CN})_6]_\infty$	Reddish brown	30.15 (30.00)	3.63 (3.80)	8.20 (8.03)	4.67 (4.61)
17	$[(4'\text{-H-stp})(\text{Me}_3\text{Sn})_3\text{Ru}(\text{CN})_6]_\infty$	Canary green	36.86 (36.74)	4.37 (4.26)	10.38 (10.12)	–
18	$[(4'\text{-OCH}_3\text{-stp})(\text{Me}_3\text{Sn})_3\text{Ru}(\text{CN})_6]_\infty$	Pale green	36.96 (36.87)	4.45 (4.40)	10.06 (9.72)	–

coordination polymers [28]. The products **1–12** (Table 1) are finally washed with chloroform to remove the unreacted materials and dried under vacuum at 30°C.



The encapsulated polymer **6** was also prepared by mixing equimolar amounts of methanolic solutions of 1-methyl-4-(4'-OCH₃-styryl) pyridinium iodide and **I**. The reaction mixture was left for 2 h in the dark under nitrogen with continuous stirring at room temperature. The orange precipitate was filtered off and washed several times with methanol and then dried in vacuo at 30°C.

The molecular species **13–18** were prepared by ion exchange reactions. Addition of equimolar quantities of each of the coordination polymers **III–VI** suspended in an aqueous methanolic solution to the stpi-salt (1) or (3) dissolved in methanol gave **13–18** (Table 2) after 3 h stirring at room temperature and leaving the reaction mixture overnight. The coloured solid precipitates were filtered off, washed with water and then with methanol and dried under vacuum at 40°C.

All the analytical and spectroscopic methods as well as the instruments are described elsewhere [28].

3. Results and discussion

3.1. Structure, chemical properties and thermal stability of the coordination polymers

The coordination polymers **I** and **II** are obtained as paramagnetic yellowish orange precipitates (μ_{eff} ; ca. 2.18 and 2.11 BM, respectively). The lead derivatives have lower thermal stability (decompose above 180°C) and

higher solubility in polar solvents than the tin derivatives (decompose above 220°C). The white coordination polymers **III–VI** are diamagnetic and thermally stable up to 300°C.

The coordination polymers **I**, **II**, **IV** and **VI** are isostructural samples as indicated by the X-ray powder diagrams (Fig. 1). Their structural features are established by studying the single crystal X-ray diffractions of the coordination polymers $[(\text{Me}_3\text{E})_3\text{Co}(\text{CN})_6]_\infty$ (E = Sn or Pb) [9,10,12] which are the homologues of and isostructural with **I** and **II** as they belong to the fundamental type $[(\text{R}_3\text{E})_3\text{M}^{\text{III}}(\text{CN})_6]_\infty$. Also, the coordination polymers **III–VI** can be considered as members of the family of the organotin^{IV} coordination polymers $[(\text{Me}_3\text{Sn})_4\text{Fe}(\text{CN})_6-4\text{H}_2\text{O}]_\infty$, $[(\text{Me}_3\text{Sn})_4\text{Fe}(\text{CN})_6-2\text{H}_2\text{O}-\text{C}_4\text{H}_8\text{O}_2]_\infty$ and $[(\text{Me}_3\text{Pb})_4\text{Fe}(\text{CN})_6-2\text{H}_2\text{O}]_\infty$ studied by single crystal X-ray diffractions as well as solid-state NMR spectra [13–15,29,30]. These studies indicated the presence of two- or three-dimensional network due to the presence of trigonal-bipyramidal (tbp) $-\text{C}=\text{N}-\overset{\text{E}}{\underset{\text{N}}{\text{C}}}-\text{C}(\text{E}=\text{Sn or Pb})$ bridges between the single d-transition metal ion ^dM. The most significant structural features of the 3D-network are the presence of two different chains with each ^dM atom as a joint member of three intersecting chains; while one-third of all chains are strictly linear, the other two-thirds display alternately two different E–N–C angles that are both smaller than 180°C. These chains display ample, straight channels with a cross-section of about 10×10 Å capable of encapsulating voluminous guest cations.

The solid-state ¹¹⁹Sn and ¹³C NMR spectra of the coordination polymers **III–VI** (Table 3) confirm the presence of two chemically different (Me₃E) groups where at most one of the four (Me₃E) groups undergoes quantitative ion exchange [9,10,12,31–33]. These groups have six crystallographically different methyl carbon setwise equivalent around room temperature owing to rapid rotation about their individual trigonal axes [9,10,12]. The network involves also three equally abundant nonequivalent CN ligands.

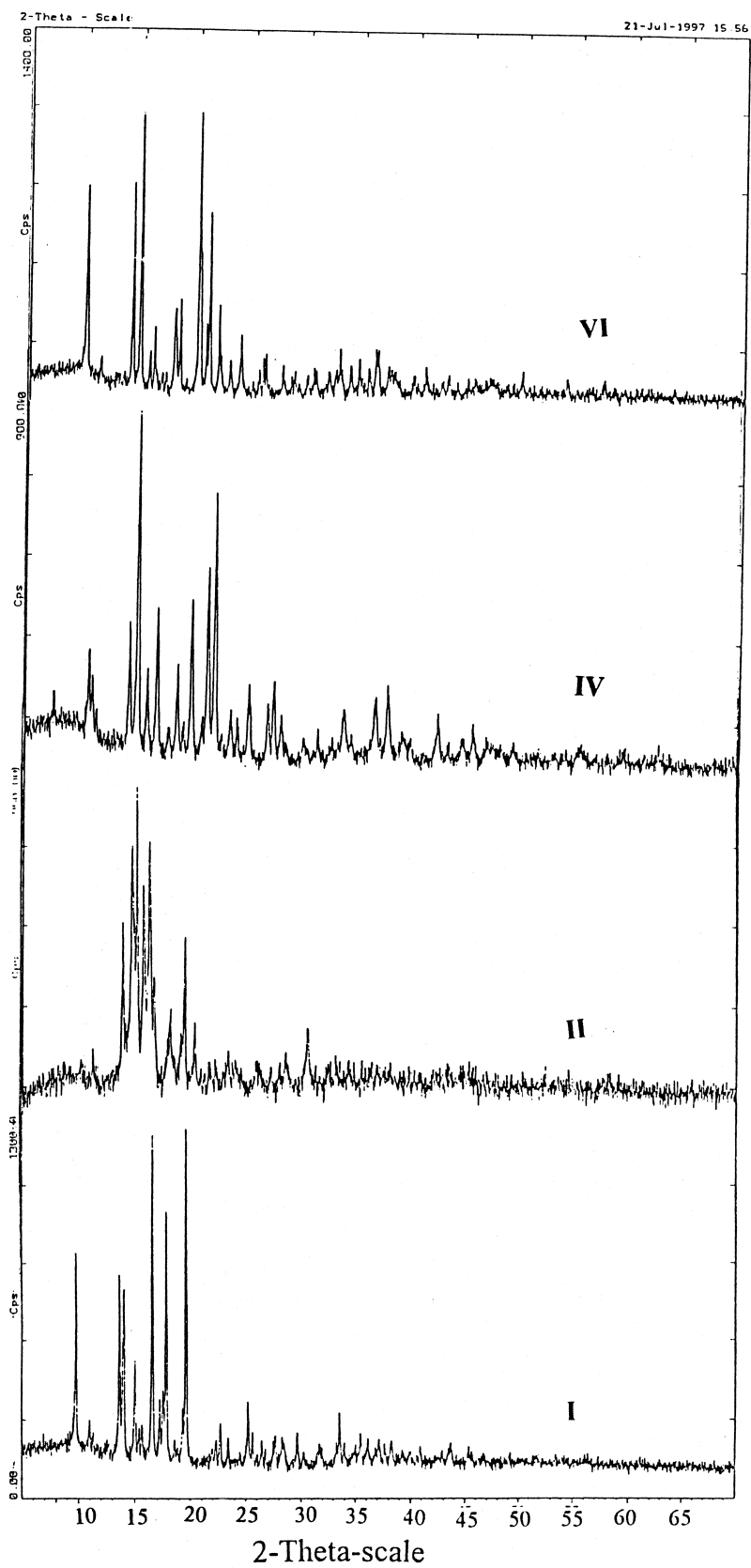


Fig. 1. X-ray powder diffraction of the coordination polymers I, II, IV and VI.

Table 3
Solid-state NMR data [9,12,30–33] ^{13}C and ^{119}Sn , for **III–VI**

No.	Coordination polymer	$\delta^{13}\text{C}/\text{ppm}$ (methyl)		$\delta^{119}\text{Sn}$ ppm	$\delta^{13}\text{C}/\text{ppm}$ (cyanide)
		-60°C	20, 40°C		
III	$[(\text{Me}_3\text{Pb})_4\text{Fe}(\text{CN})_6 \cdot 2\text{H}_2\text{O}]_\infty$		17.8, 18.1 19.24	–	167–188
IV	$[(\text{Me}_3\text{Sn})_4\text{Fe}(\text{CN})_6]_\infty$	+8.9, +3.8, +2.8 +1.5, –2.5	+4.4 +1.2	–108 +46	178, 175, 169
V	$[(\text{Me}_3\text{Sn})_4\text{Ru}(\text{CN})_6]_\infty$	+9.2, +4.4, +2.8 +2.4, 1.4, –2.1	+4.3 +1.4	–97 +32	166, 163 159
VI	$[(\text{Et}_4\text{N})(\text{Me}_3\text{Sn})_3\text{Fe}(\text{CN})_6]_\infty$	+53.6 ^a , +9.17, +6.6 +2.9, +1.0	–	–157.6 –181.3	170.5 174.6

^a $\delta^{13}\text{C}/\text{ppm}$ (Ethyl).

The IR and Raman spectra of the coordination polymers **I–VI** reveal the presence of $[\text{M}(\text{CN})_6]$ building blocks and the different (Me_3E) units (Figs. 2 and 3). The IR spectra display, mainly, two strong bands in the ν_{CN} region. However, one of these bands tends, in some cases, to split into two bands. The positions of these bands reflect the covalent nature of the $\text{M}-\text{C}\equiv\text{N}\rightarrow\text{E}$ bridging unit since

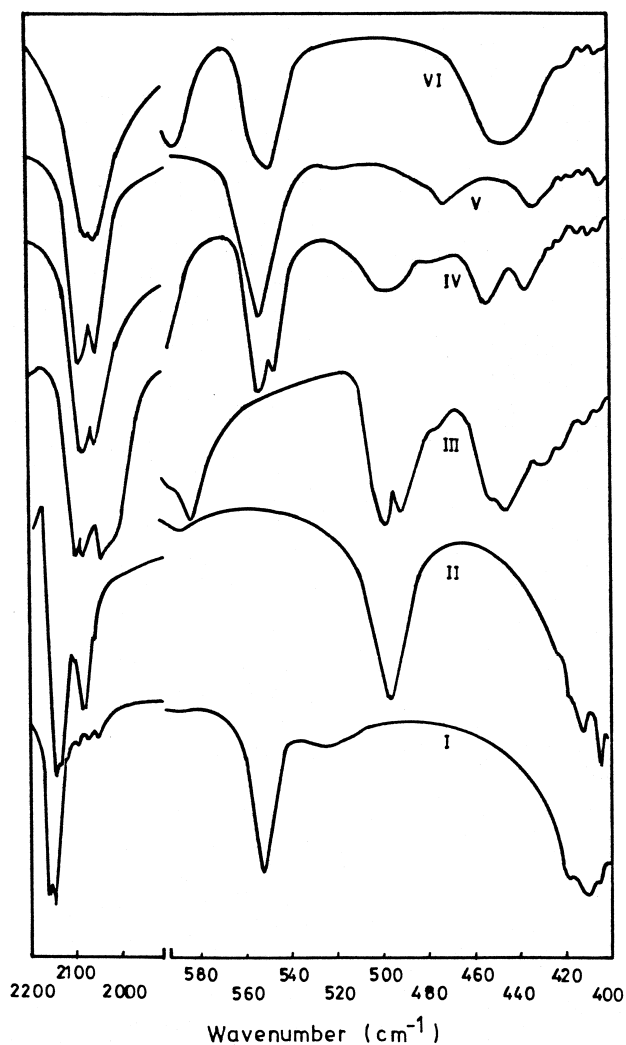


Fig. 2. IR spectra of the coordination polymers **I–VI**.

they occur usually at higher wave numbers than the ν_{CN} bands of the corresponding salts [ca. $\nu_{\text{CN}} = 2116 \text{ cm}^{-1}$ and $2072, 2043, 2025 \text{ cm}^{-1}$] for $\text{K}_3\text{Fe}(\text{CN})_6$ and $\text{K}_4\text{Fe}(\text{CN})_6$. On the other hand, the Raman spectra show three absorption bands indicating the presence of three nonequivalent CN ligands. In the $\nu_{\text{E}-\text{C}}$ region, two IR bands for **I** appear at 527 cm^{-1} ($\nu_{(\text{Sn}-\text{C})\text{sy.}}$) and 552 cm^{-1} ($\nu_{(\text{Sn}-\text{C})\text{asy.}}$). The IR band due to $\nu_{\text{pb}-\text{C}}$ of **II** appears as a broad one at 497 cm^{-1} . On the other hand, the $(\nu_{(\text{E}-\text{C})\text{asy.}}$) band of **III–V** splits into two bands with no more than 9 cm^{-1} difference while the Raman ($\nu_{(\text{E}-\text{C})\text{sy.}}$) and ($\nu_{(\text{E}-\text{C})\text{asy.}}$) bands of **III–VI**

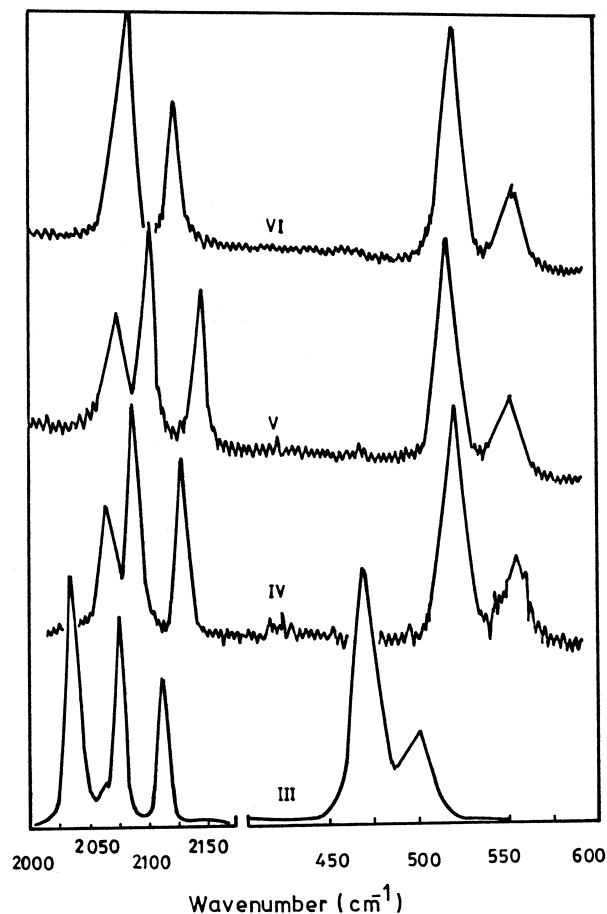


Fig. 3. Raman spectra of the coordination polymers **I–VI**.

Table 4
Vibrational frequencies (cm^{-1}) of **I–VI**

Compound	ν_{CN}		$\nu_{\text{E-C}}$		ν_{MC}
	IR	Raman	IR	Raman	
I ^a	2145, 2155		527 ^{wb} , 552		410 ^b
II ^a	2166, 2120		497 ^b		412 ^b
III	2011, 2057,	2037, 2077	491, 499	471 ^b	446
	2071	2114	518 ^w	501 ^b	451
IV	2050, 2074	2067, 2091	518 ^w , 547	520 ^b	437
		2133	552	555 ^b	454
V	2049, 2084	2076, 2102	519 ^w , 546	517 ^b	433
		2147	553 ^s	551 ^b	472
VI	2052, 2065	2075, 2082	518 ^w , 550	520 ^b	448 ^b
		2124		553 ^b	

^a Nujol mull; ^w weak; ^b broad; ^s strong.

appear at the expected positions (Table 4). These results reveal the presence of $\text{tbp-} \text{Me}_3\text{E}(\text{NC})_2$ units as well as the (Me_3E) cations. Also, the absence of the symmetric vibrations in the IR spectra of **II–VI** and the

low intensity of the Raman ($\nu_{(\text{Sn-C})_{\text{asy.}}}$) band advocate the presence of trigonal planar (Me_3E) units which are axially anchoring to two cyanide N atoms [34]. The broad appearance of the $\nu_{\text{M-C}}$ band (IR spectra of **I**, **II** and **VI**) and the presence of two split bands in the IR spectra of **III–V** support the presence of two different $[-\text{NC-M-CN-E-NC-}]$ chains with ^dM surrounded octahedrally by six cyanide ligands as gathered from the X-ray and NMR results.

3.2. The electronic absorption spectra of the coordination polymers

The electronic absorption spectra of the metal ion with d^5 configuration in the (${}^2\text{T}_{2g}$) coordination polymers **I** and **II** as Nujol mull matrix reveal five intense bands at 220, 260, 300, 320 and 440 nm (Table 5 and Fig. 4). These bands are also observed at similar positions in the diffuse

Table 5
The electronic absorption spectra of the coordination polymers **I–VI** as Nujol mull matrices and diffuse reflectance

Coordination polymer	M→L ${}^2\text{T}_{2g}(\pi) \rightarrow {}^4\text{t}_{1u}(\pi^*)$	L→M CT_1 ${}^2\text{T}_{1u}(\sigma)$	L→M CT_2 ${}^2\text{T}_{2u}$	d-d ${}^2\text{A}_{2g} \rightarrow {}^2\text{T}_{1g}$	L→M CT_3 ${}^2\text{T}_{1u}(\pi)$
	I	225, (220)	260, (258)	300, (300)	320, (320)
II	220, (222)	258, (258)	300, (305)	320, (322)	445, (460)
	CT ${}^1\text{A}_{1g} \rightarrow {}^1\text{T}_{1u}$	d-d ${}^1\text{A}_{1g} \rightarrow {}^1\text{T}_{2g}$	d-d ${}^1\text{A}_{1g} \rightarrow {}^1\text{T}_{1g}$	${}^1\text{A}_{1g} \rightarrow {}^3\text{T}_{1g}$	
III	220, (220)	250 ^b , (258)	300 ^b , (305)		
IV	225, (222)	250, (260)	325 ^b , (330 ^b)	440 ^w	
V	220, (220)	240, (255)	300 ^b , (310)		
VI	220, (222)	245 ^b , (260)	320 ^b , (320)	440 ^w	

^b broad; ^w weak.

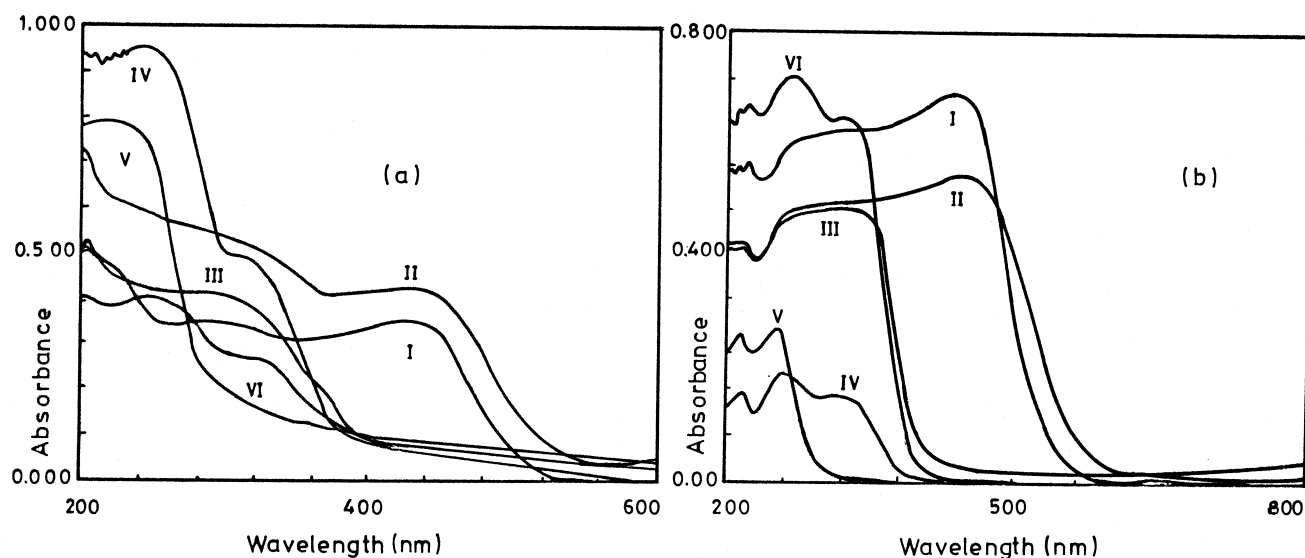


Fig. 4. Electronic spectra of the coordination polymers **I–VI** as: (a) Nujol mull matrix; and (b) diffuse reflectance.

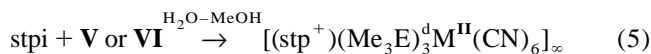
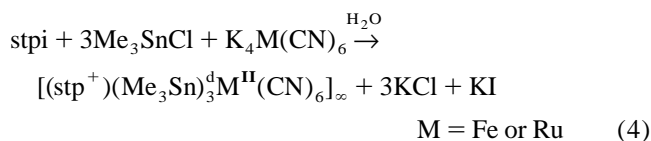
reflectance spectra. They resemble the bands observed in the absorption spectrum of $K_3[Fe(CN)_6]$ at 219, 258, 300, 318, 333 and 419 nm [35]. The first band at 220 nm is due to $\pi-\pi^*$ transitions from the metal to the cyanide ligand ($M \rightarrow L$ band). The three bands at 260, 300 and 440 nm have been identified as charge transfer transitions from the filled bonding orbitals; mainly of the cyanide ligand, to the hole in the shell of the central metal ion. They have been assigned as ${}^2T_{1u}(\sigma) \rightarrow {}^2T_{2g}$, ${}^2T_{2u}(\pi) \rightarrow {}^2T_{2g}$ and ${}^2T_{1u}(\pi) \rightarrow {}^2T_{2g}$, respectively [35]. Apart from these intense charge transfer bands, one band of low intensity is observed at 320 nm due to ligand field (d–d) transitions (${}^2A_{2g} \rightarrow {}^2T_{1g}$). The other bands due to (d–d) transitions (ca. 285 and 370 nm) [35,36] are obscured by the more intense broad bands due to $L \rightarrow M$ transitions.

The electronic absorption spectra of the $Fe(II)$ ions with d^6 configuration (${}^1A_{1g}$) in the coordination polymers **III**–**VI** as Nujol mull matrix exhibit mainly three absorption bands at 220–225, 240–250 and 300–325 nm which have the same features of the spectra of $K_4Fe(CN)_6$ and $K_4Ru(CN)_6$ [36,37], Table 5 and Fig. 4. The second and the third bands display slight red shift (ca. 255–260 and 305–330 nm) in the diffuse reflectance spectra. The last two bands at 250 and 320 nm are assigned to (d–d) transitions ${}^1A_{1g} \rightarrow {}^1T_{2g}$ and ${}^1A_{1g} \rightarrow {}^1T_{1g}$, respectively [36]. The intense band at 220 nm is due to charge transfer transition of the type ${}^1A_{1g} \rightarrow {}^1T_{1u}$ ($M \rightarrow L$ band).

The very weak band was supposed to appear at 422 nm, as observed in the spectrum of $K_4[Fe(CN)_6]$ [36] due to the first spin-forbidden transition; ${}^1A_{1g} \rightarrow {}^3T_{1g}$, appears at 440 nm in the diffuse reflectance spectra of **IV** and **VI** while it is obscured in the spectra of **III** and **V** under the more intense broad band at 320 nm.

3.3. Analytical data and thermal stability of the molecular composites

The results of chemical analysis (Table 1) reveal that the stp-cations are encapsulated within the cavities of the polymers **I** and **II** in molar ratios < 1 exhibiting zeolite like host–guest systems $[(stp)_x(Me_3E)_3Fe^{III}Fe^I(CN)_6]_\infty$ ($0 < x < 1$). These encapsulating polymers are formed by tribochemical reactions at room temperature. In this case, the iodide anion functions as an electron donor and partially reduces the host matrix, hence facilitating accommodation of the stp-cation. However, complete reduction of Fe^{III} could not be achieved even with continuous grinding and leaving the reaction mixture for several days. On the other hand, the molecular composites $[(stp^+)(Me_3E)_3M^II(CN)_6]_\infty$; **13**–**18**, can be prepared by following two different preparative routes; coprecipitation from solution Eq. (4) and by ion exchange. At most one (Me_3E^+) cation from the network of the polymers **III**–**V** or the (Et_4N^+) cation of **VI** was replaced by one stp-cation, Eq. (5).



The results of chemical analysis reveal in addition, that several samples contain solvent molecules amounting to one or two. This is further supported by DTA thermograms which show an endothermic peak at 180–220°C and TGA analysis which indicate that one or two solvent molecules release out the network of the encapsulated polymers at 160–210°C. Although, the significance of presence of the solvent molecules in the network of these encapsulated compounds, rather than considering it as adsorbed solvent, is not quite clear at the present time, it is worth noting that the presence of a few drops of water enhance significantly the rate of encapsulation, the case which has been previously observed for some other encapsulated polymers [19]. Also, the X-ray study of the supramolecular host–guest system $[(n-Bu_4N)(Me_3Sn)_2Fe(CN)_6-H_2O]$ indicated that the H_2O molecules belong at least in part, to the 3D-host framework [38].

The molecular composites are thermally stable, and photo-stable compared to the corresponding polymers [28]. The host polymers became thermally stable and photo-stable when the stp are present as guest cations in the cavities rather than the (Me_3E^+) cations. The encapsulated polymer **6** exhibits thermochromic behavior since the colour changes reversibly from orange to red on heating at 60°C (Fig. 5). The DTA thermograms indicate the decomposition of these encapsulating polymers by two exothermic peaks within the temperature range 350–540°C. The X-ray powder diffraction of the encapsulated coordination polymers **13**–**18** indicate that they are isostructural compounds to the corresponding coordination polymers.

3.4. The IR spectra of the molecular composites

The IR spectra of the molecular composites reveal that the bands are due to the 3D-host matrices and the stp-guest cations (Tables 6 and 7). The presence of the solvent molecules in the lattice of the encapsulated polymers was further supported by the appearance of the broad band at $3410-3446\text{ cm}^{-1}$ due to ν_{OH} . The presence of the weak band at $2119-2135\text{ cm}^{-1}$ and the strong broad band below 2100 cm^{-1} indicates partial transformation of the $[Fe^{III}(CN)_6]$ building blocks to $[Fe^II(CN)_6]$ to give zeolite like 3D-host–guest polymers. Under high resolution in the ν_{CN} range, the IR spectra of **2**, **3**, **5**, **7**, **8** and **10** display two bands below 2100 cm^{-1} reflecting the significantly perturbed surroundings of the Me_3E -interlinked $[Fe(CN)_6]$ octahedra. However, the absence of the bands due to, ν_{CN}

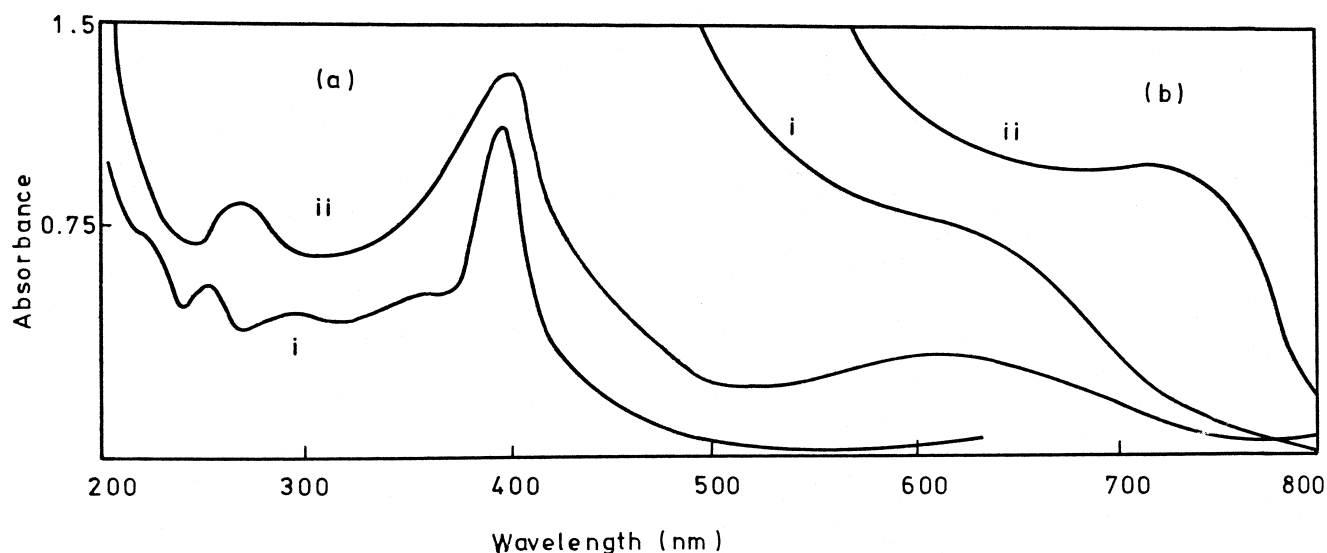


Fig. 5. Electronic spectra of the encapsulated polymer **6**: (a) absorption spectra in Nujol mull; and (b) diffuse reflectance spectra: (i) orange; (ii) red.

Table 6

The IR spectra (cm^{-1}) of the molecular composites **1–12**

Compound	$\nu_{\text{H}_2\text{O}}$	$\nu_{\text{C}\equiv\text{N}}$	(stp ⁺) cation				$\nu_{\text{E}-\text{C}}$	$\nu_{\text{Fe}-\text{C}}$
	ν_{OH}		$\nu_{\text{C}\equiv\text{N}}^{\text{a}}$	$\nu_{\text{C}=\text{C}}$	$\nu_{\text{C}-\text{N}}$	γ_{CH}		
1	3437	2123 ^w , 2051 ^b	1634	1617–1513	1207	967	549, 535	460, 448, 410 ^w
2	3420	2130 ^w , 2065, 2018	1638	1615–1510	1210	960	498, 490	456, 450, 418 ^w
3	3433, 3226	2119 ^w , 2062, 2022	1641	1622–1517	1208	968	548, 538	462, 450, 412 ^w
4	3446	2128 ^w , 2054 ^b	1642	1617–1514	1208	987	551 ^b	470, 451, 410 ^w
5	3430	2132 ^w , 2070, 2040	1640	1618–1510	1210	972	500, 489	446, 430, 414 ^w
6	3420	2055 ^b	1640	1616–1515	1208	985	550 ^b	470, 452
7	3433	2120 ^w , 2071, 2048	1639	1620–1530	1210	953	560, 553	453 ^b , 410 ^w
8	3439	2130 ^w , 2074, 2050	1643	1622–1518	1212	962	558, 551	450 ^b , 410 ^w
9	3438	2130 ^w , 2048 ^b	1639	1617–1513	1218	965	552 ^b	449 ^b , 408 ^w
10	3410	2135 ^w , 2076, 2055	1680	1620–1525	1220	960	550, 540	450 ^b , 410 ^w
11	3435, 3230	2120 ^w , 2058 ^b	1640	1614–1510	1230	978	552 ^b	448 ^b , 412 ^w
12	3430	2125 ^w , 2060	1640	1618–1531	1214	965	550 ^b	450 ^b , 410 ^w

^a Overlapped with $\delta\text{H}_2\text{O}$.

^b broad; ^w weak.

of the $[\text{Fe}^{\text{III}}(\text{CN})_6]$ building blocks in the IR spectrum of **6** indicates that the stp-cation is introduced quantitatively within the channels of the host polymer producing thermochromic encapsulated polymer. On the other hand, the appearance of two or three IR active bands in the spectra of **15–18** (Fig. 6), apart from one additional shoulder at

2104 cm^{-1} in the spectra of **16** and **17**, supports the presence of three nonequivalent CN ligands of distorted octahedral structure. The ν_{CN} bands of **13–18** occur at higher wave numbers than the bands of the corresponding host polymers reflecting more covalent interaction between the cyanide N atoms and the (Me_3E) connecting units under the effect of the nature of the guest cation. The wavenumber of the ν_{CN} band increases along the sequence $\text{Me}_3\text{pb}^+ < \text{Me}_3\text{Sn}^+ < 4'\text{-OCH}_3\text{-stp}^+ < 4'\text{-H-stp}^+$.

The characteristic bands of the stp-guest cations (Table 6) exhibit shifts to higher wave numbers relative to the bands of the stpi, indicating the presence of charge transfer from the negative host framework to the stp-cations as indicated by the diffuse reflectance spectra.

The $\nu_{\text{Fe}-\text{C}}$ vibrations, of **1–12**, except **6**, reflect clearly the presence of both the $[\text{Fe}^{\text{III}}(\text{CN})_6]$ and $[\text{Fe}^{\text{II}}(\text{CN})_6]$ building blocks while the broad appearance of both $\nu_{\text{E}-\text{C}}$ and $\nu_{\text{Fe}-\text{C}}$ bands or their splitting into two bands reflect the

Table 7

The IR spectra (cm^{-1}) of the molecular species **13–18**

Compound	$\nu_{\text{C}\equiv\text{N}}$	$\nu_{\text{E}-\text{C}}$	$\nu_{\text{M}-\text{C}}$
13	2090, 2055	560, 551 ^b , 537	460, 447
14	2055 ^b	549 ^b , 540, 519	476, 447
15	2104, 2067, 2060, 2016	508, 495, 485	456 ^b
16	2104, 2070, 2038 ^b	499 ^b , 491 ^b	445, 431
17	2104, 2094, 2061	560, 551, 535	482, 412
18	2100, 2090, 2057	550 ^b , 540	480, 420

^b broad.

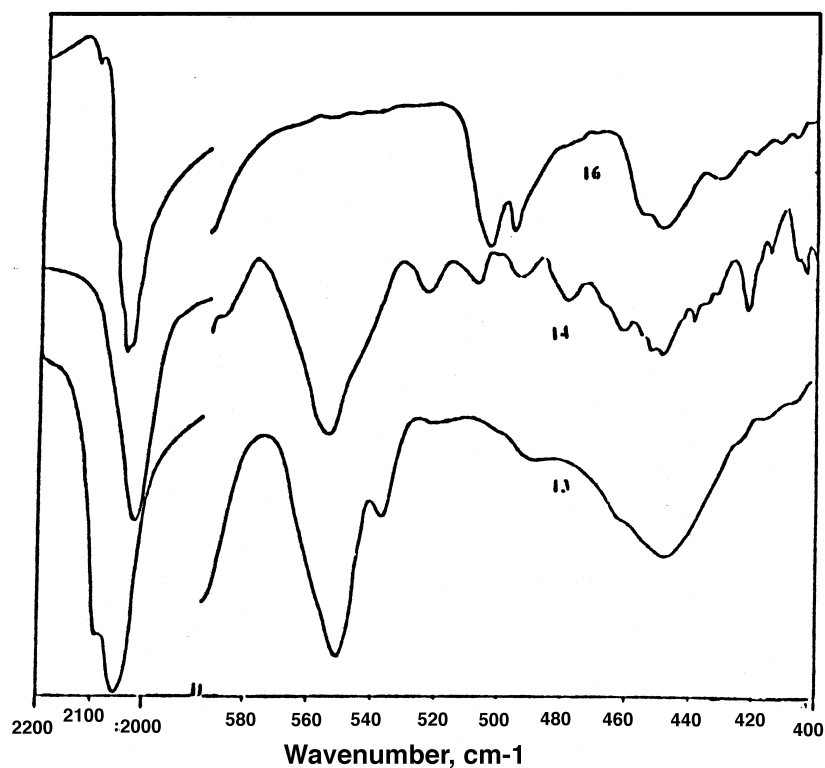


Fig. 6. High-resolution IR spectra of **13–18** in the ν_{CN} and ν_{MC} stretching regions.

presence of two nonequivalent $\text{Me}_3\text{E}(\text{NC})_2$ units (Table 6). This is further supported by the splitting of the band due to ($\nu_{(\text{E}-\text{C})_{\text{asy.}}}$) of **13–18** into two bands, and the presence of the band due to ($\nu_{(\text{Sn}-\text{C})_{\text{sy.}}}$) at around 537 cm^{-1} and that of ($\nu_{(\text{Pb}-\text{C})_{\text{sy.}}}$) at 485 cm^{-1} (Fig. 6 and Table 7). Thus, from these IR spectroscopic features, it is evident that the exchange of (Me_3E^+) cations by the stp-cations does not affect the local symmetries of the $[\text{M}(\text{CN})_6]$ building blocks.

3.5. The electronic absorption spectra of the molecular composites

The spectra of **1–12** as Nujol mull matrices reveal that the bands are due to both the stp-cations and the coordination polymers (Table 8). The broad bands at 216–225, 240–256 and 340–410 nm are attributed to $\pi-\pi^*$ transitions of the stp-guest cations in addition to transitions due to ${}^1\text{A}_{1\text{g}} \rightarrow {}^1\text{T}_{1\text{u}}$ and ${}^1\text{A}_{1\text{g}} \rightarrow {}^1\text{T}_{2\text{g}}$ of the polymers, respec-

Table 8

The electronic absorption spectra of **1–12** as Nujol mull matrices and diffuse reflectance as well as the magnetic moments

Compound	stp			Molecular species					μ_{eff}	
	$\pi-\pi^*$ transitions			$\pi-\pi^*$ transitions of stp and		${}^1\text{A}_{1\text{g}} \rightarrow {}^1\text{T}_{1\text{g}}$	CT_3	CT^{a}		BM
				${}^1\text{A}_{1\text{g}} \rightarrow {}^1\text{T}_{1\text{u}}$	${}^1\text{A}_{1\text{g}} \rightarrow {}^1\text{T}_{2\text{g}}$					
1	225	240	347	225	240	340	290	440	525	0.30
2				225	242	342	295	437	522	0.70
3	218	260	410	220	256	410	290	442	564	0.35
4	220	260	345	220	253	390	288	440	655	0.36
5	220	260	345	222	255	345	295	442	657	0.70
6	220	260	345	222	254	390	290	–	658	–
7	–	240	340, 430	220	240	340	300	445	725	0.33
8	218	240	350	220	247	352	290	440	565	0.40
9	220	260	355	220	248	350	295	435	560	0.51
10	218	240	340	218	–	340	–	435	678	0.47
11	215	255	340, 390	218	252	385	295	442	500	0.32
12	215	258	336, 380	216	255	380	290	440	510	0.31

^a Diffuse reflectance.

tively. The bands due to π - π^* transitions of the stp-guest cations appear at more or less the same positions of the stp-salts (Fig. 7). The composite band around 300 nm corresponds to d-d transitions, ${}^1A_{1g} \rightarrow {}^1T_{1g}$ of the $[\text{Fe}^{\text{II}}(\text{CN})_6]$ building blocks [37] and to charge transfer transition (CT_2 , ${}^2T_{2u} \rightarrow {}^2T_{2g}$) within the $[\text{Fe}^{\text{III}}(\text{CN})_6]$ building blocks. The weak band at 435–445 nm can be attributed to CT_3 , ${}^2T_{1u}(\pi) \rightarrow {}^2T_{2g}$ of the $[\text{Fe}^{\text{III}}(\text{CN})_6]$ building blocks. These bands support the presence of mixed valence iron hexacyano building blocks as also indicated by the weak paramagnetic behavior of these composites (Table 8). On the other hand, the diffuse reflectance spectra exhibit an additional broad band at 500–725 nm (Fig. 7), corresponding to ion-pair charge transfer (CT) between the negatively charged cavity of the host polymer and the stp-cations [39,40]. Thus, the encapsulation of the guest stp-cations within the 3D-host channels can be explained in terms of an ionic charge transfer model. On the other hand, the electronic absorption spectra do not show any bands in the near-IR region corresponding to an inter valence transition, indicating localized interaction between the mixed valence iron [41].

The electronic absorption spectra of orange **6** exhibit the absorption bands characteristic to the different transitions

of 1-methyl-4-(4⁻methoxy-styryl) pyridinium cation as well as those of the host coordination polymer (Fig. 5). The band due to CT_3 disappears while the diffuse reflectance spectrum reveals a broad band at 658 nm corresponding to the ion pair CT. On the other hand, the spectrum of the red sample displays an additional band at 620 nm which disappears on cooling the sample where the colour changes from red to orange. This band appears at 745 nm in the diffuse reflectance spectrum exhibiting blue shift on cooling.

The electronic absorption spectra of **13–16** exhibit the same bands of **1–12** except those of $[\text{Fe}^{\text{III}}(\text{CN})_6]$ building blocks while the ion-pair CT band appears at longer wavelengths. The absence of the $[\text{Fe}^{\text{III}}(\text{CN})_6]$ building blocks is further supported by the diamagnetic behavior of these encapsulated polymers. Some bands due to d-d transitions and the L \rightarrow M charge transfer bands are obscured by the more intense bands of the stp-guest cations located at the same positions. The electronic absorption spectra of **17** and **18** (Table 9) indicate that at most one of the (Me_3Sn^+) cations is exchanged quantitatively by the stp-cation which encapsulates within the channels of the negatively charged coordination polymer $[(\text{Me}_3\text{Sn})_3\text{Ru}(\text{CN})_6]_{\infty}^-$.

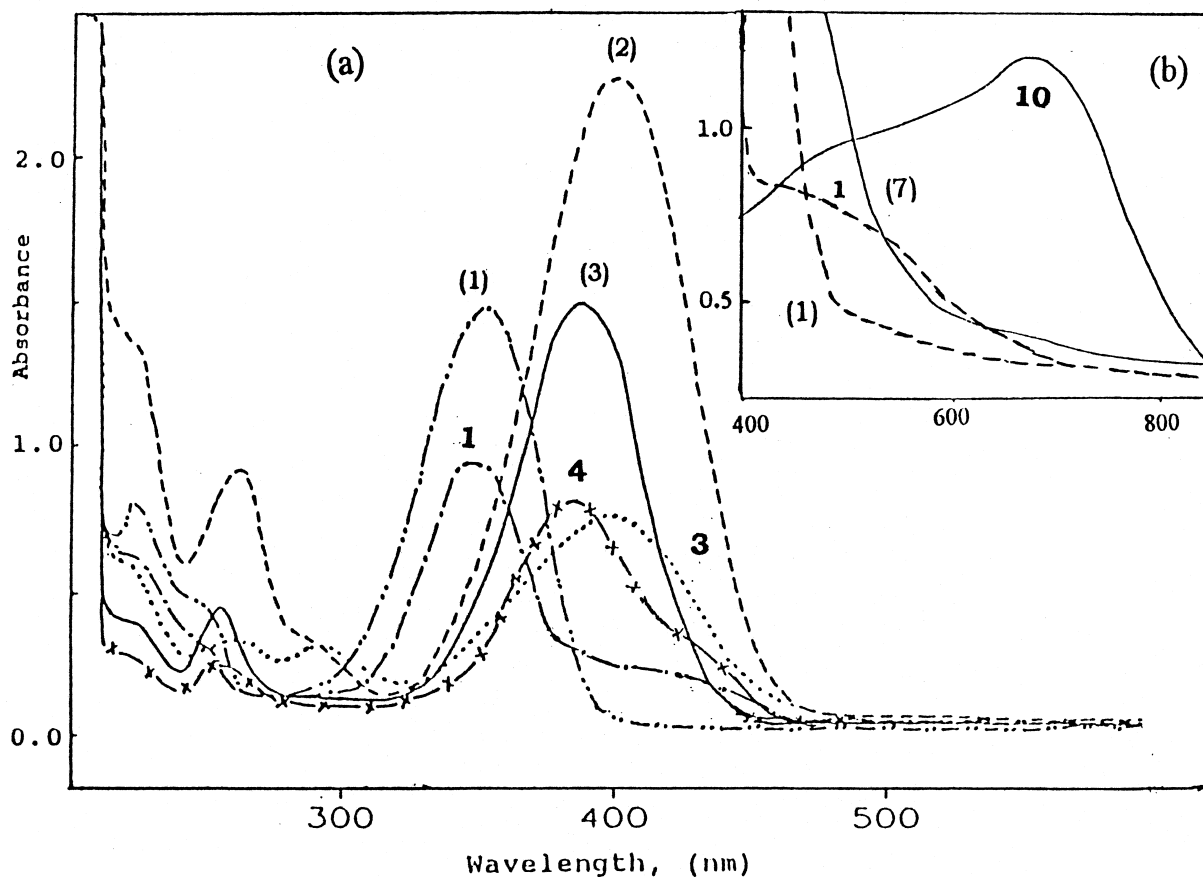


Fig. 7. (a) Electronic absorption spectra of stpi (1), (2) and (3) and the corresponding encapsulated polymers **1**, **3** and **4**. (b) Diffuse reflectance spectra of (1), (7), **1** and **10**.

Table 9

The electronic absorption spectra of **13**–**18** as Nujol mull matrices and diffuse reflectance

Compound	$\pi-\pi^*$ transition of stp and			${}^1A_{1g} \rightarrow {}^1T_{1g}$	CT ^a
	${}^1A_{1g} \rightarrow {}^1T_{1u}$	${}^1A_{1g} \rightarrow {}^1T_{2g}$			
13	222	245	340	320	530
14	225	250	390	315	670
15	220	244	338	295	532
16	220	252	392	300	675
17	222	240	340	300	526
18	220	244	385	295	569

^a Diffuse reflectance.

References

- [1] A.J. Jacobson, in: M.S. Whittingham, A.J. Jacobson (Eds.), *Intercalation Chemistry*, Academic Press, New York, 1982, p. 229, and references therein.
- [2] G.V. Subba Rao, M.W. Shafer, in: F. Levy (Ed.), *Intercalated Layered Materials*, Reidel, Dordrecht, 1979, p. 99.
- [3] T.R. Halbert, in: M.S. Whittingham, A.J. Jacobson (Eds.), *Intercalation Chemistry*, Academic Press, New York, 1982, p. 375, and references therein.
- [4] M.D. Lind, *Acta Crystallogr., Sect. B* 26 (1970) 1058.
- [5] Y. Maeda, M. Yamashita, H. Ohshio, N. Tsutsumi, Y. Takashima, *Bull. Chem. Soc. Jpn.* 55 (1982) 3138.
- [6] R.H. Herber, *Acc. Chem. Res.* 15 (1982) 216.
- [7] S.M. Kaulzarich, J.L. Stanton, J. Faber Jr., B.A. Averill, *J. Am. Chem. Soc.* 108 (1986) 7946, and references therein.
- [8] J.F. Bringley, B.A. Averill, *Chem. Mater.* 2 (1990) 181.
- [9] K. Yünlü, N. Hock, R.D. Fischer, *Angew. Chem.* 97 (1985) 865.
- [10] K. Yünlü, N. Hock, R.D. Fischer, *Angew. Chem., Intl. Ed. Engl.* 24 (1985) 873.
- [11] D.C. Apperley, A. Davies, R.K. Harris, A.K. Brimah, S. Eller, R.D. Fischer, *Organometallics* 9 (1990) 2672.
- [12] U. Behrens, A.K. Brimah, T.M. Soliman, R.D. Fischer, D.C. Apperley, N.A. Davis, R.K. Harris, *Organometallics* 11 (1992) 1718.
- [13] S. Eller, P. Schwarz, A.K. Brimah, R.D. Fischer, D.C. Apperley, N.A. Davis, R.K. Harris, *Organometallics* 12 (1993) 3232.
- [14] P. Schwarz, S. Eller, E. Siebel, T.M. Soliman, R.D. Fischer, D.C. Apperley, N.A. Davis, R.K. Harris, *Angew. Chem.* 108 (1996) 1611.
- [15] P. Schwarz, S. Eller, E. Siebel, T.M. Soliman, R.D. Fischer, D.C. Apperley, N.A. Davis, R.K. Harris, *Angew. Chem., Intl. Ed. Engl.* 35 (1996) 1525.
- [16] M. Hassanen, S.H. Etaiw, *Eur. Polim. J.* 29 (1993) 47.
- [17] A.M.A. Ibrahim, S.H. Etaiw, T.M. Soliman, *J. Organomet. Chem.* 430 (1992) 87.
- [18] S.H. Etaiw, A.M.A. Ibrahim, *J. Organomet. Chem.* 456 (1993) 229, and references therein.
- [19] A.M.A. Ibrahim, T.M. Soliman, S.H. Etaiw, R.D. Fischer, *J. Organomet. Chem.* 468 (1994) 93, and references therein.
- [20] S. Eller, M. Adam, R.D. Fischer, *Angew. Chem.* 102 (1990) 1157.
- [21] S. Eller, M. Adam, R.D. Fischer, *Angew. Chem., Intl. Ed. Engl.* 29 (1990) 1126.
- [22] S. Eller, P. Brandt, A.K. Brimah, P. Schwarz, R.D. Fischer, *Angew. Chem.* 101 (1989) 1274.
- [23] S. Eller, P. Brandt, A.K. Brimah, P. Schwarz, R.D. Fischer, *Angew. Chem., Intl. Ed. Engl.* 28 (1989) 1263.
- [24] S.T. Abdel-Halim, *J. Chem. Soc., Faraday Trans.* 89 (1993) 55.
- [25] H. Ephardt, P. Fromherz, *J. Phys. Chem.* 93 (1989) 7717.
- [26] M.J. Minch, S. Sadig Shah, *J. Chem. Edu.* 54 (1977) 709.
- [27] D.A. Evans, P.J. Jimenez, M.J. Kelly, *J. Electroanal. Chem.* 163 (1984) 145.
- [28] S.H. Etaiw, A.M.A. Ibrahim, *J. Organomet. Chem.* 522 (1996) 77.
- [29] M. Adem, A.K. Brimah, X.F. Li, R.D. Fischer, *Inorg. Chem.* 29 (1990) 1595.
- [30] A.K. Brimah, P. Schwarz, R.D. Fischer, N.A. Davies, R.K. Harris, *J. Organomet. Chem.* 568 (1998) 1.
- [31] R.K. Harris, A. Sebald, D. Furlani, G. Tagliavini, *Organometallics* 7 (1988) 388, and references therein.
- [32] R.K. Harris, A. Sebald, *Magn. Reson. Chem.* 27 (1989) 81.
- [33] M. Newcomb, J.H. Horner, M.T. Blanda, P.J. Squattrito, *J. Am. Chem. Soc.* 111 (1989) 6294.
- [34] R.J.J. Clark, A.G. Davis, R.J. Puddephalt, *J. Am. Chem. Soc.* 90 (1968) 6923.
- [35] H.H. Schmidtke, G. Evring, *Z. Physik. Chem. Neue Folge* 92S (1974) 211, and references therein.
- [36] R. Gale, A.J. McCaffery, *J. Chem. Soc.* (1973) 1344.
- [37] J.J. Alexander, H.B. Gray, *J. Am. Chem. Soc.* 90 (1967) 4260.
- [38] E. Siebel, P. Schwarz, R.D. Fischer, *Solid State Ionics* 101–103 (1997) 285.
- [39] H. Kisch, *Comments Inorg. Chem.* 16 (1994) 133.
- [40] H. Sakaguchi, T. Nagamura, T. Matsuo, *J. Chem. Soc., Chem. Commun.* (1992) 209.
- [41] C.T. Dziobkowski, J.T. Wroblewski, D.B. Brown, *Inorg. Chem.* 20 (1981) 679.